



Modeling the second solar spectrum

An empirical approach

M. Sampoorna

Instituto de Astrofísica de Canarias, E-38205 La Laguna, Tenerife, Spain.
e-mail: sampoorna@iac.es

Abstract. We present an empirical approach to model the wing polarization of strong resonance lines. This procedure based on 'last scattering approximation' (LSA) was developed by Stenflo (1980, 1982), for coherent scattering in the laboratory frame. We generalize his empirical approach to handle partial frequency redistribution (PRD). We illustrate this approach by applying it to the Ca I 4227 Å line. The LSA approach is successful in reproducing the observed Stokes Q/I polarization, including the location of the wing polarization maxima and the minima around the Doppler core, but fails to reproduce the observed spatial variations of the far wing polarization in terms of magnetic field and PRD effects. This null result points in the direction of a non-magnetic origin, which may include local deviations from a plane-parallel stratification with an inhomogeneous solar atmosphere.

Key words. line: formation – magnetic fields – polarization – scattering – Sun: atmosphere

The linearly polarized spectrum of the Sun (Second Solar Spectrum), is formed by scattering of anisotropic radiation on the bound states of atoms and molecules. The modification to this non-magnetic scattering by magnetic fields produces what is called Hanle effect.

The largest degree of linear polarization in the visible solar spectrum is exhibited by the strong resonance Ca I 4227 Å line (Stenflo, 1982). Recent observations by Bianda et al. (2003) in this line showed for the first time spatial variations of the linear polarization (Q/I and U/I) in the far line wings, which pointed to the possible existence of wing Hanle effect. These observations made in active regions is in contradiction with established fact that the Hanle ef-

fect should only be effective in the line core but not in the line wings, where it should approach the non-magnetic resonance scattering limit (see Omont et al., 1973; Stenflo, 1994; Landi Degl'Innocenti & Landolfi, 2004). Here we present further such observations, this time done in quiet regions. Again we find similar spatial variations in the line wings, which we refer to as the “(Q/I , U/I) wing signatures”.

We examine the magnetic origin for these wing signatures. It may be possible if elastic collisions are able to cause sufficient frequency redistribution to make the Hanle effect show up in the wings without causing excessive collisional depolarization, as suggested by recent theories for partial frequency redistribution (PRD) in magnetic fields (see Nagendra et al., 2002, 2003; Sampoorna et al., 2007a,b). In this

Send offprint requests to: M. Sampoorna

paper we explore the above suggestion, using the last scattering approximation (LSA) instead of full radiative-transfer modeling. The results presented in this paper are discussed in greater detail in Sampoorna et al. (2009).

1. Observations

Spectropolarimetric recordings of the full Stokes vector were obtained using the 45 cm aperture Gregory Coudé Telescope (GCT) at IRSOL (Locarno, Switzerland) and the ZIMPOL-2 polarimeter system. In total 86 positions at different limb distances and at various latitudes on the solar disk were recorded, with the spectrograph slit parallel to the limb (which defines the positive Stokes Q direction).

Spatially varying linear polarization structures in the wings (of Stokes Q and/or U) are found in approximately half of all our recordings. We illustrate in Fig. 1 a representative example. The spectrograph slit width was 125 microns, which corresponds to $1''$, and its length corresponded to about $170''$.

In the top panel, the Q/I profile shown by the solid line is obtained by averaging outside the interval where depolarization in the line wings is observed, while the dashed line represents the profile obtained by averaging in the interval ($55'' - 75''$) where depolarization is seen. The difference between the two averaged Q/I profiles is shown by the $\Delta(Q/I)$ line.

In the bottom panel of Fig. 1 the solid line represents the U/I profile averaged over the spatial interval $29'' - 40''$. Its shape resembles a negative version of the Q/I profile. The absence of large signals in V/I shows that we are observing a solar region where very weak longitudinal magnetic field components exist.

2. Theoretical model based on LSA

Quantitative modeling of the scattering polarization in Ca I 4227 Å line requires the solution of the radiative transfer problem taking into account PRD (see Holzreuter et al., 2005, and references cited therein). For exploratory purposes we can avoid such full-scale radiative transfer modeling by using semi-empirical

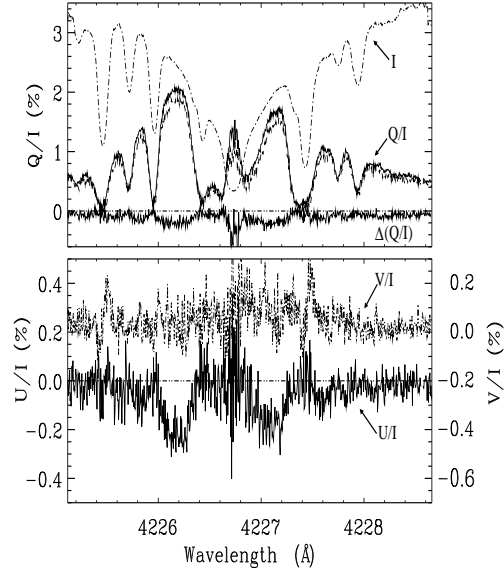


Fig. 1. Observed Stokes I , Q/I , U/I , V/I profiles. The heliocentric angle corresponds to $\mu = 0.1$. Note the depolarization in the Q/I wings and the U/I signatures at the corresponding wavelength positions. We refer to them together as the “(Q/I , U/I) wing signatures”.

approaches in terms of the LSA, which has proven successful in the past (Stenflo, 1982).

LSA exploits the fact that the polarization of the radiation that escapes the atmosphere is determined by the anisotropy of the radiation field at the place where the last scattering occurs. Since the polarization amplitudes in the lines are small, the incident radiation at the last scattering event can be assumed to be unpolarized. In other words, the emergent polarization is produced in a single scattering event (the very last one) rather than through multiple scattering within the atmosphere.

Under LSA the emergent scattering polarization in the presence of a weak magnetic field is:

$$\frac{Q}{I} = S \left[P_{Q,\text{line}} \frac{H}{H+C} + P_c \frac{C}{H+C} \right], \quad (1)$$

$$\frac{U}{I} = S P_{U,\text{line}} \frac{H}{H+C}; \quad H \equiv H(\Delta\lambda, a). \quad (2)$$

$P_{X,\text{line}}$ with $X = Q, U$ gives the contribution of line to the linear polarization Q/I or U/I . LSA allows us to write them in the form

$$P_{X,\text{line}} = \frac{\int R_{i1}(\lambda, \lambda', \Theta) k_{G,\lambda}(\mu) I_{\lambda'}(\mu = 1) d\lambda'}{\int R_{11}(\lambda, \lambda', \Theta) I_{\lambda'}(\mu = 1) d\lambda'} \quad (3)$$

Here, when $X = Q, U$, we have $i = 2, 3$ respectively. For the scattering redistribution matrix elements $R_{i1}(\lambda, \lambda', \Theta)$ with $i = 1, 2, 3$ we use the Hanle-Zeeman theory (Sampoorna et al., 2007a,b). R_{i1} depend on the incoming (λ') and the outgoing (λ) wavelengths, and on the scattering angle Θ . The anisotropy factor $k_{G,\lambda}(\mu)$ describes the depolarization caused by the angular integration over the incident radiation.

The Voigt function $H(\Delta\lambda, a)$ describes the absorption probability for the Ca I 4227 Å line, with damping parameter a given by

$$a = \frac{\Gamma_R + \Gamma_I + \Gamma_E}{4\pi\Delta\nu_D} = a_R \left[1 + \frac{\Gamma_I + \Gamma_E}{\Gamma_R} \right], \quad (4)$$

where $\Delta\nu_D$ is the Doppler width of the line, Γ_I , Γ_R , and Γ_E are respectively the inelastic, radiative and elastic collision rates. Since the inelastic collision rate $\Gamma_I \ll \Gamma_E$, we set $\Gamma_I = 0$. For the Ca I 4227 Å the radiative width is $\Gamma_R = 2.18 \times 10^8 \text{ s}^{-1}$. For a temperature $T = 6000 \text{ K}$ and $v_{\text{turb}} = 2 \text{ km s}^{-1}$, we have $\Delta\lambda_D = 35.9 \text{ mÅ}$, and $a_R = \Gamma_R/(4\pi\Delta\nu_D) = 2.8 \times 10^{-3}$.

For a given choice of Γ_E/Γ_R , the free parameters of our model are S , C , P_c . The global scaling parameter S is adjusted such that the amplitude of the modeled Q/I blue wing maximum agrees with the observed value. The continuum opacity parameter C allows us to reproduce the overall shape of the observed Q/I in the near and far wings of the Ca I 4227 line. In particular it determines the wavelength positions where the maximum wing polarization is reached. The continuum polarization P_c is fixed by the asymptotic behavior of Q/I far from the line center.

We calculate $k_{G,\lambda}(\mu)$ empirically using the observed limb darkening function, $c_\lambda(\mu) \equiv I_\lambda(\mu)/I_\lambda(\mu = 1)$ (see Sampoorna et al., 2009, for details). We fit this $c_\lambda(\mu)$ determined from the observed data by

$$f_\lambda(\mu) = 1 - a_{0,\lambda} - a_{1,\lambda} + a_{0,\lambda}\mu + a_{1,\lambda}\mu^2. \quad (5)$$

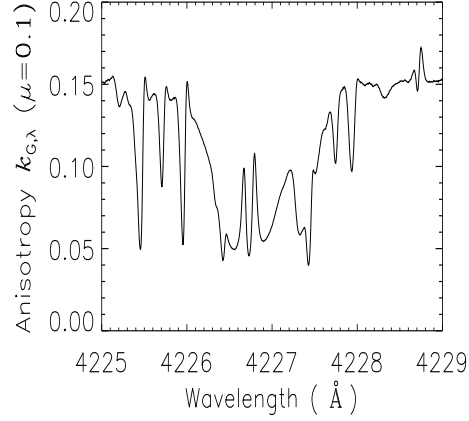


Fig. 2. Plot of the anisotropy factor $k_{G,\lambda}(\mu)$ as a function of λ for disk position $\mu = 0.1$.

Least square fitting of $c_\lambda(\mu)$ in terms of $f_\lambda(\mu)$ gives us the coefficients $a_{0,\lambda}$ and $a_{1,\lambda}$.

For use with LSA we obtain the $k_{G,\lambda}(\mu)$ by multiplying the Rayleigh phase matrix with an unpolarized Stokes vector $(I, 0, 0, 0)^T$ and integrating over all the incoming angles (see Stenflo, 1982). This allows us to obtain a simple analytic form for $k_{G,\lambda}(\mu)$, given by

$$k_{G,\lambda}(\mu) = \left(\frac{3a_{0,\lambda}}{64} + \frac{a_{1,\lambda}}{20} \right) \frac{(1 - \mu^2)}{f_\lambda(\mu)}. \quad (6)$$

Fig. 2 shows a plot of the anisotropy factor $k_{G,\lambda}(\mu)$ for $\mu = 0.1$. The resemblance of $k_{G,\lambda}(\mu)$ to the $I_\lambda(\mu)$ spectra is very striking in the far wings. However, it also has a distinctive shape in the core and wings of the Ca I 4227 Å line. $k_{G,\lambda}(\mu)$ has a minimum in both the core of the main line and the cores of the surrounding blend lines. It is largest in the line wings, where it reaches a nearly constant value.

3. Results

Figure 3 illustrates the important role played by the $k_{G,\lambda}(\mu)$, and PRD. Comparing the solid and dashed line model profiles we see that the entire structuring of the Q/I model profile, with the minima around the Ca I 4227 Å Doppler core and the blend line depressions are all related to the $k_{G,\lambda}(\mu)$ structure (see Fig. 2). The blend line minima of the model profile

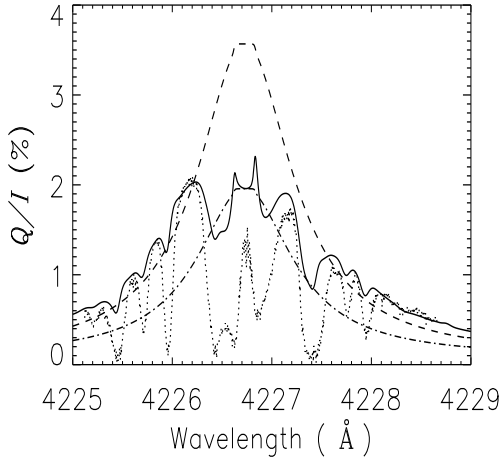


Fig. 3. Role of $k_{G,\lambda}(\mu)$ and PRD. The solid line is the model profile computed using PRD and $k_{G,\lambda}(\mu)$ found by observations. The dotted line is the observed Q/I in the non-magnetic region. The dashed line is the model profile with PRD and a flat $k_{G,\lambda}(\mu) = 0.112$. The dot-dashed line is computed using the complete redistribution (CRD) approximation and non-flat $k_{G,\lambda}(\mu)$. The free parameters are $S = 0.325$, $C = 9.7 \times 10^{-5}$ and $P_c = 0.25\%$.

(solid line) are less deep than in the observed spectrum (dotted line). This is because we have disregarded the fact that the blend line opacities can have intrinsic polarizability $W_2 = 0$ and thus dilute the Ca I 4227 line photons with unpolarized photons. Further comparing solid and dot-dashed line model profiles, we see that it is not only $k_{G,\lambda}(\mu)$ that governs the shape and magnitude of the wing maxima in Q/I , but also a realistic redistribution matrix, namely, PRD.

Comparison with the observed Q/I spectrum shows that LSA allows us to model the Q/I wings extremely well and we can fit the envelope (above the blend line depressions) of the observed Q/I . The line core of Ca I 4227 is however not modeled so well by LSA, although correct qualitative features like the Q/I dips around the Doppler core are reproduced. Clearly LSA does not work well enough in the line core, and one may need radiative-transfer physics to explain the core shape of Q/I .

Figure 4 shows our attempts to model the observed $(Q/I, U/I)$ wing signatures in terms of the wing Hanle effect. The parameters now required for the modeling are Hanle $\Gamma_B = geB/(2m\Gamma_R)$ in standard notation, and (ϑ_B, φ_B) representing the orientation of a directed magnetic field, defined with respect to the atmospheric normal. The elastic collision rate Γ_E is also used as a free parameter.

We introduce a quantity $\Delta(Q/I) = (Q/I)_{\text{mag}} - (Q/I)_{\text{non-mag}}$, which is a measure of the depolarization caused together by the magnetic field and elastic collisions. In the top panel of Fig. 1 we observe depolarization in Q/I not only in the line core, but also in the wings (compare the solid and dashed lines in that figure). Our study shows that when $\Gamma_E/\Gamma_R = 0$ we do not get any wing depolarization ($\Delta(Q/I) \approx 0$), regardless of the choice of the field parameters. However, when we introduce elastic collisions we find that for an optimum choice of the combination $(\Gamma_B, \Gamma_E/\Gamma_R)$, we do get wing depolarization ($\Delta(Q/I) \neq 0$) in Q/I . For example, when $(\Gamma_B, \Gamma_E/\Gamma_R) = (10, 10)$ we observe Hanle depolarization that extends into the wings as shown in Fig. 4 (compare the heavy solid and the thin solid lines), but no wing peaks are obtained in $\Delta(Q/I)$ that is represented by the dashed line.

Our modeling turns out to be unsuccessful in reproducing the observed wing maxima in $-U/I$, contrary to our expectations. We expected that the elastic collisions play a significant role in transferring the Hanle effect from the line core to the line wings without destroying the atomic polarization (Nagendra et al., 2003; Bianda et al., 2003; Sampoorna et al., 2007b). This expectation is satisfied to some extent for Q/I for an optimum choice of $(\Gamma_B, \Gamma_E/\Gamma_R)$, but even in this optimized case we fail to reproduce the wing maxima that are seen in the observed $\Delta(Q/I)$.

4. Conclusions

The LSA gives excellent fit to the linear polarization that is observed in the wings of spectral lines, as demonstrated for the case of the Ca I 4227 Å line. The most important quantity in our modeling is the anisotropy factor $k_{G,\lambda}(\mu)$,

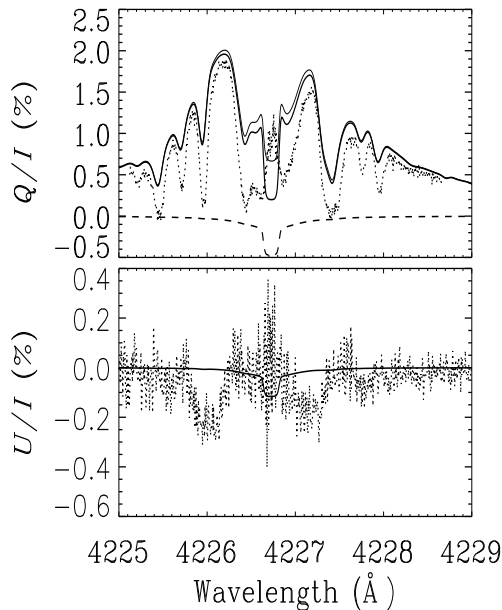


Fig. 4. Attempt to model the (Q/I , U/I) wing signatures. The observations (dotted lines) shown here correspond to the “magnetic observations” in Fig. 1. In the Q/I panel the heavy solid line represents the magnetic model profile, the thin solid line the non-magnetic model profile, and the dashed line their difference. In the U/I panel the solid line represents the magnetic model profile. The parameters used are $(\Gamma_B, \vartheta_B, \varphi_B; \Gamma_E/\Gamma_R) = (10, 90^\circ, 135^\circ; 10)$.

which we determine from the observed center-to-limb variation of the Stokes I spectrum. The detailed wavelength variation of the limb-darkening function plays a fundamental role and is responsible in particular for the occurrence of Q/I minima that surrounds the core region and separates it from the wing maxima. Another key ingredient is the appropriate partial frequency redistribution matrix to be used.

Our attempts to model the observed spatial variations in the Q/I and U/I wings of the Ca I 4227 Å line in terms of the Hanle effect, were unsuccessful. This null result appears to rule out a direct magnetic-field origin (via the Hanle effect), in contradiction to earlier suggestions (Nagendra et al., 2003; Bianda et al., 2003; Sampoorna et al., 2007b), at least within

the framework of the currently available PRD theory. This points in the direction of a non-magnetic interpretation, such as local deviations from a plane-parallel stratification with an inhomogeneous solar atmosphere containing “hot spots” (Holzreuter & Stenflo, 2007; Trujillo Bueno & Shchukina, 2007).

Acknowledgements. I thank IAU for a grant, which helped me to participate in the IAU General Assembly held in Rio de Janeiro in 2009. I acknowledge the financial support by the Spanish Ministry of Science through project AYA2007-63881.

References

- Bianda, M., Stenflo, J. O., Gandorfer, A., & Gisler, D. 2003, in ASP Conf. Ser. 286, Current Theoretical Models and Future High Resolution Solar Observations: Preparing for ATST, eds. A. A. Pevtsov & H. Uitenbroek (San Francisco: ASP), 61
- Holzreuter, R., Fluri, D. M., & Stenflo, J. O. 2005, A&A, 434, 713
- Holzreuter, R., & Stenflo, J. O. 2007, A&A, 472, 919
- Landi Degl’Innocenti, E., & Landolfi, M. 2004, Polarization in Spectral Lines (Kluwer Academic Publishers)
- Nagendra, K. N., Frisch, H., & Faurobert, M. 2002, A&A, 395, 305
- Nagendra, K. N., Frisch, H., & Fluri, D. M. 2003, in ASP Conf. Ser. 307, Solar Polarization, ed. J. Trujillo Bueno & J. Sanchez Almeida (San Francisco: ASP), 227
- Omont, A., Smith, E. W., & Cooper, J. 1973, ApJ, 182, 283
- Sampoorna, M., Nagendra, K. N., & Stenflo, J. O. 2007a, ApJ, 663, 625
- Sampoorna, M., Nagendra, K. N., & Stenflo, J. O. 2007b, ApJ, 670, 1485
- Sampoorna, M., Stenflo, J. O., Nagendra, K. N., Bianda, M., Ramelli, R., & Anusha, L. S. 2009, ApJ, 699, 1650
- Stenflo, J. O. 1980, A&A, 84, 68
- Stenflo, J. O. 1982, Sol. Phys., 80, 209
- Stenflo, J. O. 1994, Solar Magnetic Fields (Kluwer Academic Publishers)
- Trujillo Bueno, J., & Shchukina, N. 2007, ApJ, 664, L135